Magnetism in Compressed Fullerenes

The Origin of the Magnetic Moments in Compressed Crystals of Polymeric C_{60}**

*Jordi Ribas-Ariño and Juan J. Novoa**

Makarova et al.[1] reported that the rhombohedral phases of polymeric C_{60} (*rh*-C_{60}) exhibit the typical properties of ferromagnets (magnetization hysteresis loops, saturation magnetization) up to 500 K, and this is a remarkable and puzzling performance for a purely organic molecular magnet (the previous highest critical temperature at atmospheric pressure was 36 K,[2] which increased to 65 K on applying a pressure of 16 kilobars[3]). These findings were later confirmed by Wood et al.[4] on pristine C_{60} at 9 GPa and 800 K. The origin of magnetism in *rh*-C_{60} still lacks a solid explanation based on evidence, although the original authors suggested some possibilities. Here, on the basis of results from quantum-mechanical calculations, it is shown that under pressure the lowest energy state for a pair of 2+2 covalently linked C_{60} molecules is a triplet T_2 state with only one

---

[*] J. Ribas-Ariño, Prof. J. J. Novoa
Departament de Química Física
Facultat de Química and CER Química Teòrica
Parc Cientific, Universitat de Barcelona
Av. Diagonal 647, 08028-Barcelona (Spain)
Fax: (+34) 93-402-1231
E-mail: novoa@qf.ub.es

[**] This work was sponsored by the CEPBA-IBM Research Institute, as one of its cooperative research projects. We also thank the Spanish "Ministerio de Ciencia y Teconología", and the Catalan CIRIT for grants which made this work possible (projects BQU2002-04587-C02-02 and 2001SGR-0044, respectively). J.R. also acknowledges Universitat de Barcelona and "Ministerio de Educación Cultura y Deportes" for the award of a Ph.D. grant.

Supporting information for this article is available on the WWW under http://www.angewandte.org or from the author.

DOI: 10.1002/ange.200352118

interfragment C–C bond, in which the C_{60} molecules are doublets. Once formed at high pressure/temperature, the T_2 state is stable at ambient pressure, and radical centers can be found in the solid. When enough activated bonds are present in the solid, it can exhibit macroscopic magnetic properties.

At room temperature, the nonmagnetic *rh*-C_{60} phases form stacks of hexagonal planes (Figure 1).[6,7] In each plane the C_{60} molecules are joined to six neighboring C_{60} molecules by two C–C single bonds with a length of 1.68 Å.[6] Each pair of bonds results from a [2+2] cycloaddition involving one [6,6] bond (at the junction of two hexagons) in each C_{60} molecule.[8–10] No precise structural information is available on the structure of *rh*-C_{60} samples under pressure and at high temperature, although all evidence supports preservation of the C_{60} units and the presence of a layered structure.[1,4]

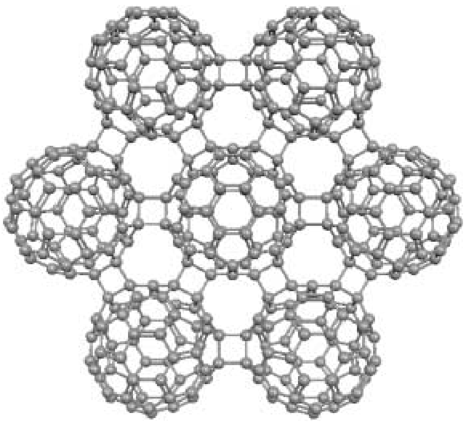

Figure 1. Structure of the planes of rhombohedral polymeric C_{60}.

The origin of the magnetic interactions[11] in compressed *rh*-C_{60} is puzzling. Experimental data excluded that magnetism is due to O_2 adsorbed on the samples or the presence of small amounts of impurities.[1,4,12] Recent experimental data[4] also ruled out that the magnetic properties could be due to radical fragments formed by rupture of C_{60} molecules under the external pressure (the experiments showed that the formation of magnetic *rh*-C_{60} phases does not damage the C_{60} molecules). Therefore, we are left with what was considered by Palacio[13] to be "the most basic and obvious question": where do the magnetic moments in compressed *rh*-C_{60} come from? Some proposals were put forward by the original authors,[1,4] without giving any solid evidence for their validity. This prompted us to carry out a systematic exploration, using quantum-chemical methods, of the changes undergone by C_{60}–C_{60} bonds when they are compressed, by searching for stable open-shell states.

Our main line of approach was that, at the macroscopic level, compression decreases the macroscopic volume, which, at the microscopic level, translates into a shortening of the intermolecular C_{60}–C_{60} bonds. Therefore, the possible structural and electronic changes induced by the external pressure in these bonds can be investigated by studying the shape of the potential energy curve of the C_{60}–C_{60} bonds in the short-distance region. In a first approach, we can explore the changes in the simplest model representing C_{60}–C_{60} bonds of the *rh*-C_{60} planes, namely, the unsubstituted C_{60}–C_{60} dimer. These calculations were performed with the B3LYP density functional,[14] as implemented in a parallel version of GAMESS.[15]

The existence of magnetic interactions requires the presence of thermally accessible open-shell states. Therefore, we explored the shape of the potential energy curves for the most stable singlet (S_0), triplet (T_1), and quintet (Q_1) states (the geometry of the dimer was fully optimized at each point; in the S_o T_1 and Q_1 states the two C–C interfragment bonds are forced to be equal). To lower the computational cost we explored the curves in two steps: a full search was performed for a "half-ball" model of the C_{60}–C_{60} dimer; then, selective calculations on the whole C_{60}–C_{60} dimer were carried out on the physically relevant regions of the curves. The half-ball model is a $C_{32}H_{10}$–$C_{32}H_{10}$ dimer obtained by removing one hemisphere from each ball of the C_{60}–C_{60} dimer along the equator and adding C–H bonds to equatorial C atoms where C–C bonds were present before the cut. It is designed to mimic the electronic structure in the [6,6] C atoms participating in the [2+2] cycloaddition (the optimum geometry of both dimers exhibit the same distribution of double and single bonds around the [6,6] C atoms, and the distances are similar (see Supporting Information). Both dimers were oriented as in the *rh*-C_{60} planes, the preferred orientation for the [2+2] cycloaddition of two C_{60} molecules.[16,17]

Figure 2 shows the shape of the lowest energy singlet (S_0), triplet (T_1), and quintet (Q_1) potential energy curves calculated for the $C_{32}H_{10}$–$C_{32}H_{10}$ dimer by using the B3LYP functional and the 3-21G basis set. The curves range from a longest C–C interfragment distance of 4 Å to a distance of 1.1 Å, for which the interaction energy is on the order of 300 kcal mol^{-1}. The compression of two isolated half-balls in their singlet S_0 ground state leads to formation of a doubly

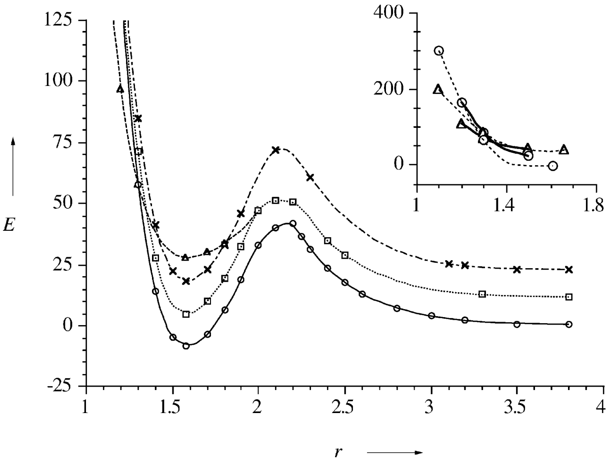

Figure 2. Potential energy curves for the $C_{32}H_{10}$–$C_{32}H_{10}$ dimer in the singlet S_0 (circles), triplet T_1 (squares), triplet T_2 (triangles), and quintet Q_1 states (crosses). Inset: S_0 and T_2 curves for the C_{60} dimer in the region of S_0–T_2 crossing, calculated at the B3LYP/3-21G and BLYP/plane wave levels (broken and solid lines, respectively). The energy E is given in kcal mol^{-1}, and the C–C interfragment distance r in angstroms.

C–C covalently linked $C_{32}H_{10}$–$C_{32}H_{10}$ dimer after overcoming an activation barrier of about 40 kcal mol^{-1} (the structure of the $C_{32}H_{10}$–$C_{32}H_{10}$ dimer and the activation barrier are similar to those found for compression of two C_{60} molecules[18,19]). Each half of the $C_{32}H_{10}$–$C_{32}H_{10}$ dimer (Figure 3) has the electronic structure of an isolated $C_{32}H_{10}$(singlet), with alternating single and double bonds, with the exception of the [6,6] bonds involved in the [2+2] cycloaddition. When higher pressure is applied, the $C_{32}H_{10}$–$C_{32}H_{10}$ dimer is forced to climb the repulsive wall of the S_0 curve, where it crosses the curve of the triplet T_2 state, but not the T_1 or Q_1 curves.

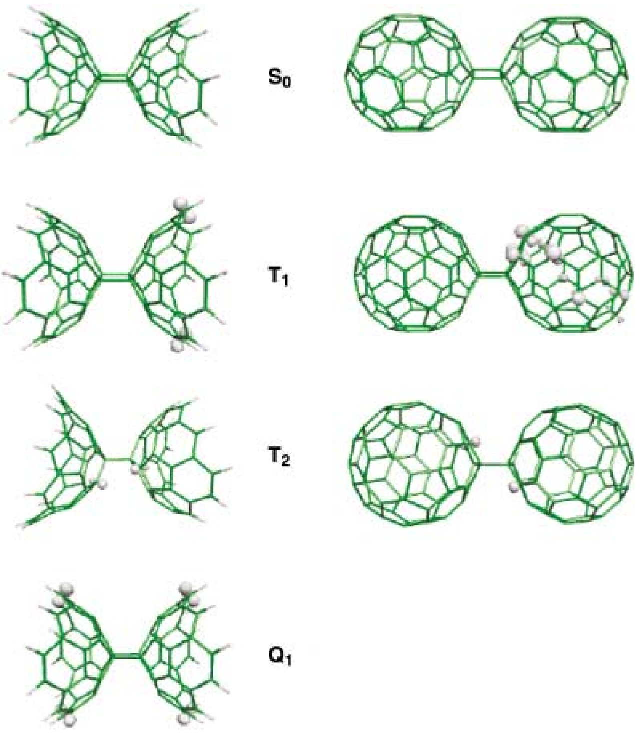

Figure 3. Optimum geometry of the S_0, T_1, T_2, and Q_1 states of the $C_{32}H_{10}$–$C_{32}H_{10}$ and C_{60}–C_{60} dimers. The spin distribution of some states is also shown (the 0.045 a.u. surface, a region of high spin distribution).

The lowest energy triplet (T_1) and quintet (Q_1) states are obtained by taking the S_0 state and converting C=C double bonds to C–C bonds without destroying the topology of the balls (T_1 dissociates into a $C_{32}H_{10}$(triplet) and a $C_{32}H_{10}$(singlet) fragment, while Q_1 dissociates into two $C_{32}H_{10}$(triplet) fragments). The T_1 and Q_1 curves are nearly parallel to the S_0 curve at interfragment distances larger than the minimum, and their minimums lie at similar C–C interfragment distances (1.586, 1.586, and 1.587 Å, for the S_0, T_1, and Q_1 states, respectively). This is an indication of similar electronic structures of the $C_{32}H_{10}$(singlet) and $C_{32}H_{10}$(triplet) fragments in the region of the [6,6] bonds involved in the [2+2] cycloaddition. As the S_0, T_1, and Q_1 curves never cross (Figure 2) the T_1 and Q_1 states cannot be responsible for the existence of magnetic interactions in compressed pristine C_{60} crystals.

The state responsible for the presence of magnetic interactions in the half-ball dimers is the T_2 triplet state. It is obtained when one of the two interfragment C–C bonds present in the S_0 state is broken and its two electrons are placed in a triplet disposition, one in each fragment (each $C_{32}H_{10}$ fragment of the T_2 state is a doublet). The T_2 triplet has a minimum at an interfragment C–C bond length of 1.590 Å (see Figure 2). There are two minimum-energy conformations: one in which the four [6,6] atoms involved in the [2+2] cycloaddition (C_1–C_4) are in a *trans* disposition (C1-C2-C3-C4 ca. 180°), and another in which they are in a *gauche* arrangement (C_1-C2-C3-C4 ca. 60°). In both minima the T_2 state is less stable than the S_0, T_1, or Q_1 minima (Figure 2). The transition from T_2 to S_0, T_1, or Q_1 is forbidden by the Frank–Condon principle, since the T_2 state has a rotational maximum for the C1-C2-C3-C4 dihedral angle where the S_0, T_1, and Q_1 have minima (C1-C2-C3-C4 0°). Consequently, overlap of the vibrational functions of T_2 with these of S_0, T_1, or Q_1 is negligible. The T_2 state becomes the ground state when the interfragment C–C distance is shorter than 1.3 Å, a fact that can be interpreted by stating that the energy required to compress the two fragments of the dimer is smaller when they are linked by one C–C bond than when they are linked by two. The T_2 and T_1 curves dissociate into the same fragments, that is, $C_{32}H_{10}$(singlet) and a $C_{32}H_{10}$(triplet).

Having determined the shape of the half-dimer curves, we then calculated the required points in the S_0 and T_2 curves of the C_{60}–C_{60} dimer to show the presence of a minimum in these curves and T_2–S_0 curve crossing (the minimum obtained by full optimization; the crossing by single-point B3LYP/STO-3G optimization at three points, followed by a B3LYP/3-21G calculation of the energy). The optimum geometry and spin density for the S_0, T_1, and T_2 states of the C_{60}–C_{60} dimer are shown in Figure 3. The B3LYP/3-21G C_{60}–C_{60} S_0 and T_2 curves are shown in the inset of Figure 2. We found that 1) the S_0 and T_2 curves have a minimum, 2) the optimum geometries of the C_{60}–C_{60} dimers (Figure 3) are similar to those calculated for the half-ball model (in the S_0 state the optimum interfragment C–C distance is 1.611 Å in the half-ball dimer and 1.633 Å in the C_{60}–C_{60} dimer), 3) the T_2 and S_0 curves cross around 1.3 Å, and 4) the electronic structures of the T_2 states of the C_{60}–C_{60} and half-ball dimers are similar (Figure 3). We also found that the T_2 state has two minima, for C1-C2-C3-C4 angles around 60° and 180° (the *trans* is 3.5 kcal mol^{-1} more stable than the *gauche* conformation). The existence of T_2–S_0 curve crossing was also found in DFT calculations with plane-wave basis[20] on these C_{60}–C_{60} curves around the crossing region (see inset in Figure 2). Consequently, the magnetically active species in the C_{60}–C_{60} dimers are C_{60} molecules covalently connected by one C–C interfragment bond, in which each C_{60} molecule is a doublet coupled in a ferromagnetic fashion.

The previous results can now be used to understand the generation of magnetic interactions in compressed polymeric *rh*-C_{60} phases. As the structure of these phases is not currently known, we will only perform a qualitative analysis with the help of Figure 4. After an initial pressure is applied to pristine $C_{60,}$ C_{60}–C_{60} bonds are formed in the S_0 state (light arrows in Figure 4). All electrons are paired, so these bonds are diamagnetic. When higher pressure is applied to the solid,

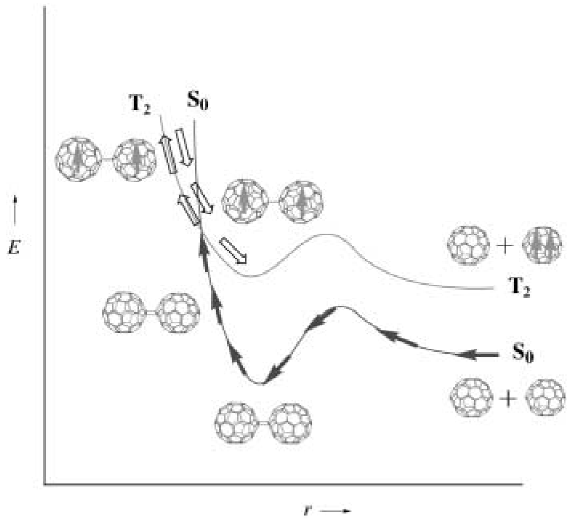

Figure 4. Graphical representation of the electronic and structural changes which take place when two C_{60} molecules in their ground state are compressed (follow the arrows). The molecules initially are on the diamagnetic S_0 surface (dark arrows). When enough pressure is applied they reach the S_0–T_2 crossing point. There, some dimers cross to the ferromagnetic T_2 state (light arrows). When the pressure decreases, these ferromagnetic dimers go back to the S_0–T_2 crossing point. Some remain on the ferromagnetic T_2 surface and reach the T_2 minimum. These bonds are magnetically active.

the C_{60}–C_{60} bonds are forced into the repulsive wall. At some point, the S_0 and T_2 curves cross, and thus some of the bonds can cross to the T_2 state and become magnetically active (dark arrows in Figure 4). Increasing the temperature makes it easier to reach the crossing point at lower pressures (by populating the appropriate excited vibrational states). When the pressure and temperature of the T_2 activated bonds is released they go down the T_2 curve. A percentage of them will remain in the T_2 state after passing through the S_0–T_2 crossing point, and thus remain magnetically active, until they reach the T_2 minimum. The percentage of molecules in the T_2 state versus the S_0 state is small, a fact that agrees with the small density of magnetic moments in these solids. The molecules can remain in the T_2 state because jumping to the T_1 or S_0 states by emission of a photon is vibrationally forbidden (the latter is also spin-forbidden).

If enough bonds remain in the T_2 state, they allow the presence of continuous paths of T_2 magnetically active bonds, and macroscopic magnetic behavior is observed. We calculated the nature of the magnetic coupling for two adjacent C_{60}–C_{60} bonds in a C_{60}–C_{60}–C_{60} trimer in which the two end C_{60} fragments are doublet radicals, and the central one is a diradical). The ground state is a quintet or a singlet, depending on the *orto*, *meta*, or *para* position of the lateral fragments, that is, adjacent T_2 bonds can couple ferro- or antiferromagnetically.[21] Studies are underway to evaluate the probability of each type of coupling and the magnitude of the magnetic interaction.

In summary, ab initio calculations on C_{60}–C_{60} dimers indicate that the magnetically active species in compressed *rh*-C_{60} solids are C_{60} molecules participating in C_{60}–C_{60} bonds that are in their T_2 state. In this T_2 state the C_{60} molecules are doublets covalently connected by one C–C interfragment bond. When enough C_{60}–C_{60} bonds are in this T_2 state, the magnetic interaction can propagate through the solid. Adjacent T_2 bonds can couple ferro- or antiferromagnetically, depending on their relative positions.

Received: June 11, 2003 [Z52118]

Keywords: ab initio calculations · fullerenes · magnetic properties

[1] T. L. Makarova, B. Sundqvist, R. Hohne, P. Esquinazi, Y. Kopelevich, P. Scharff, V. A. Davydov, L. S. Kasherova, A. V. Rakhmanina, *Nature* **2001**, *413*, 716–718.

[2] F. Palacio, G. Antorrena, M. Castro, R. Burriel, J. Rawson, J. N. B. Smith, N. Bricklebank, J. J. Novoa, C. Ritter, *Phys. Rev. Lett.* **1997**, *79*, 2336–2339.

[3] M. Mito, T. Kawae, K. Takeda, S. Takagi, Y. Matsushita, H. Deguchi, J. M. Rawson, F. Palacio, *Polyhedron* **2001**, *20*, 1509–1512.

[4] R. A. Wood, M. H. Lewis, M. R. Lees, S. M. Bennington, M. G. Cain, N. Kitamura, *J. Phys. Condens. Matter* **2002**, *14*, L385–L391.

[5] B. Sundqvist, *Adv. Phys.* **1999**, *48*, 1–134.

[6] M. Núñez-Regueiro, L. Marques, J.-L. Hodeau, O. Béthoux, M. Perroux, *Phys. Rev. Lett.* **1995**, *74*, 278–281.

[7] C. H. Xu, G. E. Scuseria, *Phys. Rev. Lett.* **1995**, *74*, 274–277.

[8] M. Prato, *J. Mater. Chem.* **2002**, *7*, 1097–1109.

[9] *The Physics of Fullerene-Based and Fullerene-Related Materials* (Ed.: W. Andreoni), Kluwer, Dordrecht, **2000**.

[10] *Acc. Chem. Res.* **1992**, *25*, 98–175, special issue on fullerenes.

[11] For a good introduction to the magnetism of molecule-based materials, see: J. S. Miller, A. J. Epstein, *Angew. Chem.* **1994**, *106*, 399; *Angew. Chem. Int. Ed. Engl.* **1994**, *33*, 385–415.

[12] R. Höhne, P. Esquinazi, *Adv. Mater.* **2002**, *14*, 753–756.

[13] F. Palacio, *Nature* **2001**, *413*, 690–691.

[14] B3LYP is a density functional obtained by taking the three-parameter nonlocal exchange funcional of Becke and the nonlocal correlation functional of Lee–Yang–Parr: A. D. Becke, *J. Chem. Phys.* **1993**, *98*, 5648–5652; C. Lee, W. Yang, R. G. Parr, *Phys. Rev. B* **1988**, *37*, 785–789.

[15] GAMESS, Revision 2000, M. W. Schmidt, K. K. Baldridge, J. A. Boatz, S. T. Elbert, M. S. Gordon, J. H. Jensen, S. Koseki, N. Matsunaga, K. A. Nguyen, S. J. Su, T. L. Windus, M. Dupuis, J. A. Montgomery, *J. Comput. Chem.* **1993**, *14*, 1347–1363.

[16] J. Kürti, K. Németh, *Chem. Phys. Lett.* **1996**, *256*, 119–125.

[17] G. E. Scuseria, *Chem. Phys. Lett.* **1996**, *257*, 583–586.

[18] Experimental data: D. V. Konarev, S. S. Khasanov, A. Otsuka, G. Saito, *J. Am. Chem. Soc.* **2002**, *124*, 8520–8521.

[19] Theoretical data on C_{60} and derivatives is reviewed in W. Andreoni, *Annu. Rev. Phys. Chem.* **1998**, *49*, 405–439.

[20] These calculations were carried out on isolated C_{60}–C_{60} dimers by using CPMD-3.5.2 (J. Hutter et al., Copyright IBM Zurich Research Laboratory and MPI für Festkörperforschung, **1995–2001**) with the BLYP functional. The cutoff value was 35 Ry. The dimer was placed in a box large enough to avoid interaction between dimers. Full details of this calculation will be given elsewhere.

[21] J. Ribas-Ariño, J. J. Novoa, *J. Phys. Chem. Solids*, accepted.